The Journal of Immunology

Azithromycin Polarizes Macrophages to an M2 Phenotype via Inhibition of the STAT1 and NF-κB Signaling Pathways

Dalia Haydar, Theodore J. Cory, Susan E. Birket, Brian S. Murphy, Keith R. Pennypacker, Anthony P. Sinai and David J. Feola

J Immunol 2019; 203:1021-1030; Prepublished online 1 July 2019;
doi: 10.4049/jimmunol.1801228
http://www.jimmunol.org/content/203/4/1021

The Journal of Immunology is published twice each month by
The American Association of Immunologists, Inc.,
1451 Rockville Pike, Suite 650, Rockville, MD 20852

Print ISSN: 0022-1767 Online ISSN: 1550-6606.

Azithromycin Polarizes Macrophages to an M2 Phenotype via Inhibition of the STAT1 and NF-κB Signaling Pathways

Dalia Haydar,*[,1] Theodore J. Cory,[†,1] Susan E. Birket,[‡] Brian S. Murphy,[§] Keith R. Pennypacker,[¶,‖] Anthony P. Sinai,[#] and David J. Feola*

Azithromycin is effective at controlling exaggerated inflammation and slowing the long-term decline of lung function in patients with cystic fibrosis. We previously demonstrated that the drug shifts macrophage polarization toward an alternative, anti-inflammatory phenotype. In this study we investigated the immunomodulatory mechanism of azithromycin through its alteration of signaling via the NF-κB and STAT1 pathways. J774 murine macrophages were plated, polarized (with IFN-γ, IL-4/-13, or with azithromycin plus IFN-γ) and stimulated with LPS. The effect of azithromycin on NF-κB and STAT1 signaling mediators was assessed by Western blot, homogeneous time-resolved fluorescence assay, nuclear translocation assay, and immunofluorescence. The drug's effect on gene and protein expression of arginase was evaluated as a marker of alternative macrophage activation. Azithromycin blocked NF-κB activation by decreasing p65 nuclear translocation, although blunting the degradation of IκBα was due, at least in part, to a decrease in IKKβ kinase activity. A direct correlation was observed between increasing azithromycin concentrations and increased IKKβ protein expression. Moreover, incubation with the IKKβ inhibitor IKK16 decreased arginase expression and activity in azithromycin-treated cells but not in cells treated with IL-4 and IL-13. Importantly, azithromycin treatment also decreased STAT1 phosphorylation in a concentration-dependent manner, an effect that was reversed with IKK16 treatment. We conclude that azithromycin anti-inflammatory mechanisms involve inhibition of the STAT1 and NF-κB signaling pathways through the drug's effect on p65 nuclear translocation and IKKβ. ***The Journal of Immunology*****, 2019, 203: 1021–1030.**

Although the function of alternatively activated macrophages (M2-polarized) has primarily been evaluated in host responses to disease processes that elicit Th2-type immune mechanisms (1–4), little is known of their role in regulating inflammation in response to extracellular Gram-negative bacterial infections. M2-polarized macrophages primarily function to orchestrate remodeling and repair by producing effector molecules such as Arginase 1 (Arg1) and TGF-β. In the cystic fibrosis lung, these mediators control lung homeostasis, inflammation, and subsequent pulmonary damage associated with pneumonia (4, 5). We have demonstrated that the antimicrobial azalide azithromycin (AZM) can induce macrophage characteristics that are consistent with M2 polarization, both in vitro and in a mouse model of *Pseudomonas aeruginosa* pneumonia (6–8). The subsequent improvement observed in the severity of lung destruction and in the mortality of this infection model has direct bearing on chronic inflammatory lung conditions, such as cystic fibrosis, in which *P. aeruginosa*–relapsing pneumonias contribute to the decline in pulmonary function over time (9, 10).

Macrophages are polarized to distinct functional phenotypes via signaling through two separate pathways (11–13). Classical, or M1 macrophages are activated by TNF-α or IFN-γ when stimulated by nonself foreign Ags (such as LPS in the case of Gram-negative bacteria) (14, 15). Signaling through IFN regulatory transcription factor and STAT is the central governing mechanism of macrophage M1-M2 polarization (14–16). LPS signaling through the pattern recognition receptor TLR4 activates several signaling cascades which involve two adaptors, MyD88 and TRIF. MyD88 signaling activates NF-κB, the main M1 macrophage transcription factor (14, 15). Alternatively, TRIF signaling promotes the secretion of type I IFNs through IFN regulatory transcription factor 3 activation. Consequently, secreted IFNs bind receptors on macrophages and stimulate the phosphorylation and activation of the second M1 transcription factor, STAT-1. Phosphorylated STAT-1 subunits form dimers and translocate to the nucleus (15), inducing the transcription of many inflammatory mediators and cytokines (12, 13).

Similarly, NF-κB activation involves a series of phosphorylation steps that result in its translocation from the cytoplasm to the nucleus. Canonical NF-κB is the prototypical proinflammatory transcription factor activated through TLR and inflammatory cytokine signaling. In the absence of TLR and cytokine receptor stimulants, NF-κB activation is suppressed by an inhibitory subunit (IκBα, IκBβ, or IκB), which binds to dimerized NF-κB subunits (p50 or RelA [also named p65]) and prevents them from translocating to their site of action in the nucleus. Therefore,

*Department of Pharmacy Practice and Science, University of Kentucky College of Pharmacy, Lexington, KY 40536; [†]Department of Clinical Pharmacy and Translational Science, University of Tennessee Health Science Center, Memphis, TN 38163; [‡]Division of Pulmonary, Allergy and Critical Care Medicine, University of Alabama-Birmingham, Birmingham, AL 35294; [§]Medpace, Cincinnati, OH 45227; [¶]Department of Neurology, University of Kentucky College of Medicine, Lexington, KY 40536; [‖]Department of Neuroscience, University of Kentucky College of Medicine, Lexington, KY 40536; and [#]Department of Microbiology, Immunology and Molecular Genetics, University of Kentucky College of Medicine, Lexington, KY 40536

[1]D.H. and T.J.C. contributed equally to this work.

ORCIDs: 0000-0002-7959-2699 (D.H.); 0000-0002-3350-8527 (T.J.C.); 0000-0002-0865-3095 (B.S.M.); 0000-0002-4618-0903 (K.R.P.); 0000-0003-1129-2304 (D.J.F.).

Received for publication September 6, 2018. Accepted for publication June 14, 2019.

This work was supported by the National Institute of Allergy and Infectious Diseases under Award Number R01AI095307 (to D.J.F.).

Address correspondence and reprint requests to Dr. David J. Feola, University of Kentucky, 789 South Limestone, Lexington, KY 40536. E-mail address: david.feola@uky.edu

The online version of this article contains supplemental material.

Abbreviations used in this article: AZM, azithromycin; BMDM, bone marrow–derived macrophage; Ct, cycle threshold; HTRF, homogeneous time-resolved fluorescence; IKK, IκB kinase; iNOS, inducible NO synthase.

stimulation through TLR, IL-1R, or other TNF receptor family members results in a series of phosphorylation reactions activating the IκB kinase (IKK) complex (a trimeric complex comprised of two catalytic subunits, IKKα and IKKβ, and a regulatory subunit, IKKγ) (17, 18). Activated IKKβ phosphorylates the NF-κB inhibitory subunit IκBα. Once phosphorylated, the IκBα subunits undergo rapid ubiquitination and proteasomal degradation, thus releasing p50/p65 from the inhibited state. Dimerized subunits then translocate to the nucleus, where they bind to the NF-κB DNA promoter region, thereby controlling several genes for proinflammatory cytokines and mediators, including TNF-α, IL-1β, IL-6, IL-12, inducible NO synthase (iNOS), and IFN-γ (19–23). Regulation of NF-κB activation mainly involves tight control of the activity and synthesis of the IκBα and IKKβ proteins (sensitive to NF-κB activation through negative feedback regulation) as well as controlling subunit nuclear translocation and DNA binding (18). Additionally, IKKβ activation requires phosphorylation of two serines; thus, regulation of IKKβ activation involves tight control of its *trans*-autophosphorylation as well as its phosphorylation by the upstream kinases (18, 20, 21).

Alternative, or M2 macrophage polarization, occurs through the binding of either IL-4 or IL-13 to their respective receptors, leading to the phosphorylation and dimerization of STAT-6. Upon activation, STAT-6 translocates to the nucleus and upregulates the expression of genes associated with anti-inflammatory processes (24–28). Through our work characterizing the effects of azithromycin (AZM), we found that the drug is only able to polarize macrophages to an M2-like phenotype when they are also stimulated with LPS (26). This characteristic provides the basis for our hypothesis that the mechanism of the drug's ability to polarize cells lies in its interference with these signaling cascades. Others have shown that AZM decreases the activation of NF-κB signaling and subsequent production of proinflammatory cytokines and other inflammatory effectors (29, 30). Although these effects alone may help to explain the beneficial effects of AZM in patients with cystic fibrosis, the mechanism by which AZM is able to polarize macrophages toward an M2-like phenotype is unknown.

In the current study we investigate the hypothesis that AZM polarizes macrophages to an M2 phenotype via inhibition of STAT-1 and NF-κB signaling mediators. We demonstrate that AZM inhibits the nuclear translocation of p65, and this correlated with concurrent increased amounts of IKKβ. Additionally, STAT-1 phosphorylation was inhibited by the drug. The addition of an IKKβ competitive inhibitor resulted in a reversal of production of the alternatively activated macrophage effector Arg1. These results provide insights into the immunomodulatory mechanism of AZM and support studies by others that demonstrate an interface between the two pathways through IKKβ.

Materials and Methods

Macrophage polarization

In vitro assays used to study AZM's mechanism of action were performed using the murine macrophage cell line J774A.1 (American Type Culture Collection, Manassas, VA) as well as using primary bone marrow–derived macrophages (BMDMs). J774 macrophages were allowed to grow and reach confluency using DMEM plus 10% FBS plus 1% sodium pyruvate plus 1% penicillin/streptomycin in all experiments. Confluent cells were scraped, counted, and plated in 24-well plates at a concentration of 2.5×10^5 cells per 1 ml of media. Cells were allowed to adhere for 4–8 h and then polarized to an M1 phenotype with IFN-γ (final concentration 20 ng/ml) or to an M2 phenotype with both IL-4 and IL-13 (final concentration 10 ng/ml of each). AZM was added to select wells along with IFN-γ at concentrations ranging from 5 to 100 μM. Additionally, IKK-16, an IKKβ inhibitor, was added to select wells with AZM and IFN-γ (final concentrations 50 or 100 nM). Cells were then incubated overnight at 37°C with 5% CO_2. Polarized cells were then stimulated with LPS (final concentration 100 ng/ml). The duration of LPS stimulation ranged from 0 to 60 min or up to 24 h, depending on the experimental goals. Cells were then washed, harvested by scraping, enumerated, and lysed in 0.1% (v/v) Triton X-100 (protease and phosphatase inhibitors were added to the lysis buffer prior to use). Protein concentrations were quantified using the Pierce BCA reaction kit. Alternatively, in some experiments, cells were fractionated into nuclear and cytoplasmic contents or homogenized with TRIzol for RNA extraction. Additionally, bone marrow cells isolated from the femur and tibia bones of sacrificed C57BL/6 mice were cultured for 6 d in RPMI 1640 supplemented with L929 supernatant containing M-CSF. After 6 d, BMDMs were plated at 2.5×10^5 cells/ml in a 24-well plate. Cells were allowed to adhere for 8 h and then polarized to an M1 phenotype or to an M2 phenotype as described above.

RNA isolation and quantitative RT-PCR

RNA isolation was performed using TRIzol Reagent (Invitrogen, Carlsbad, CA) and RNeasy Mini Kits (QIAGEN, Valencia, CA) per manufacturer's instructions. Isolated RNA was quantified using a NanoDrop 2000 spectrophotometer (Thermo Fisher Scientific, Wilmington, DE). Equal amounts of RNA were then reverse transcribed into cDNA using the iScript cDNA Synthesis Kit (Bio-Rad Laboratories, Hercules, CA) according to manufacturer's protocols. cDNA samples were then used for quantitative real-time PCR using the TaqMan gene expression arrays for murine Arg1, Ikbkb (IKKβ) and GAPDH. An epMotion 5070 robot was used to accurately pipette the PCR components (cDNA template, forward and reverse primers, TaqMan Gene Expression Master Mix, and RNase-free water) into 384-well plates. Plates were centrifuged briefly and transferred into the ABI Prism 7900HT Fast Real-Time PCR System (Applied Biosystems, Foster City, CA) set for 40 standard thermal PCR cycles. The generated cycle threshold (Ct) values were used to quantify gene expression. ΔCt values were calculated by normalizing the target gene expression (Arg1 and Ikbkb) to the housekeeping gene expression (GAPDH). The ΔΔCt was then calculated by comparing the expression of the experimental condition to the control condition. Power analysis of the generated ΔΔCt values was then used to interpret the fold change in gene expression.

RelA translocation assay

A nuclear translocation assay was used to interpret NF-κB activation by quantifying the amount of translocated p65 subunit (RelA) in the nucleus compared with that remaining in the cytoplasm. Polarized and stimulated J774 macrophages were counted and fractionated into nuclear and cytoplasmic fractions using the NF-κB Assay Kit (FIVEphoton Biochemicals, San Diego, CA) according to the manufacturer protocol. Supernatants containing the cytoplasmic and nuclear fractions were collected, and p65 was quantified in each by Western blot.

Immunofluorescence staining and analysis

Immunostaining was used to visualize the NF-κB subunit localization in stimulated cells. Macrophages were polarized as described except that round glass coverslips (12 mm) were added to each well of the 24-well plates. Cells were allowed to attach to the glass coverslips overnight. After polarization and stimulation, the coverslips were washed three times with PBS++ (PBS containing 0.5 mM $CaCl_2$ and $MgCl_2$). Cells were then fixed and permeabilized with ice-cold methanol. Primary and secondary Abs were diluted at appropriate concentrations in 3% BSA, as determined by titration experiments, and each was applied to the coverslips sequentially for 45-min incubations in a humidified chamber. The coverslips were finally incubated in DAPI nucleic acid stain (Invitrogen), washed, and mounted using an antifade reagent. Stained cells were visualized using a Zeiss fluorescent microscope (Oberkochen, Germany) with a 100× objective. Multiple fields were evaluated to score at least 150 cells per replicate coverslip by two blinded investigators. Each cell was evaluated to determine the localization of the p65 signal with respect to the nucleus as follows: p65 signal in cytoplasm only (score 0), evenly distributed between the nucleus and cytoplasm (score 1), mostly nuclear with faint cytoplasmic signal (score 2), or nuclear signal only (score 3). Scores were then averaged and compared with the control condition.

Arginase assay

Arginase enzymatic activity was assessed using the urea-based assay. Arginase is an enzyme which metabolizes arginine into ornithine and urea; therefore, urea concentrations directly correlate with the activity and expression level of arginase. J774 murine macrophages were polarized and lysed with 0.1% Triton X-100 (containing protease and phosphatase inhibitors), as described previously (6). The enzyme was activated by incubating 50 μl of the cell lysate with 50 μl of the arginase activation solution (10 mM $MnCl_2$ in 50 mM Tris HCl [pH 7.5]) for 10 min at 55°C. Subsequently, 25 μl of the mixture was added to 25 μl of

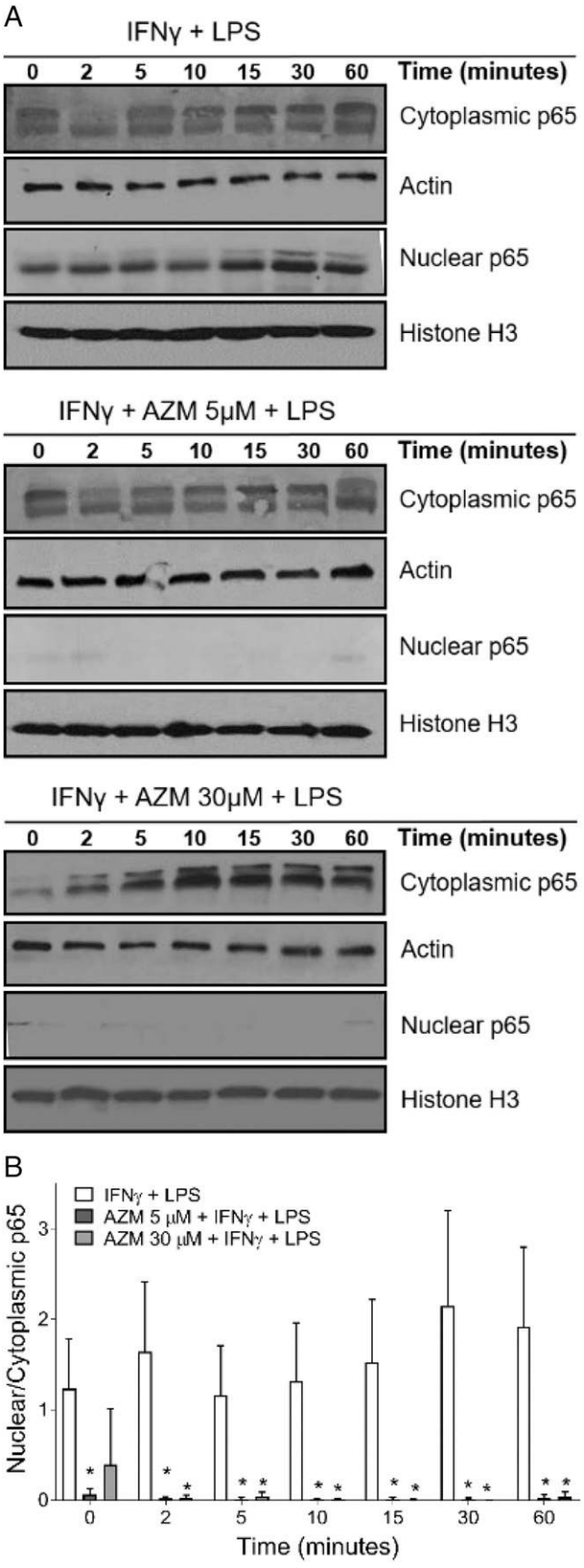

FIGURE 1. AZM decreases NF-κB activation and prevents p65 nuclear translocation. J774 cells were plated at 2.5×10^5 cells per 1 ml of media in 24-well plates. Cells were allowed to attach for 8 h and were then polarized overnight with IFN-γ (50 U/ml) alone or with AZM over a range of concentrations. Cells were then stimulated with LPS (10 nM) for durations ranging from 0 to 60 min. (**A**) Cells were harvested by scrapping, and the nuclear and cytoplasmic fractions were separated. Western blots were performed to detect p65 in nuclear and cytoplasmic fractions. (**B**) Bar graph represents the ratio of nuclear to cytoplasmic fractions of p65 from (A). Nuclear fractions are normalized to histone H3, and cytoplasmic fractions are normalized to actin. AZM-treated groups were compared with the control group. Data are depicted as mean ± SD and are representative of three independent experiments. Statistical significance was determined by two-way ANOVA with Sidak multiple comparisons test. $*p < 0.05$.

the arginase substrate solution (0.5 M L-arginine in water [pH 9.7]) and incubated at 37°C for 6 h. The reaction was then terminated by adding an acid mixture (H_2SO_4, H_3PO_4, water at a ratio of 1:3:7), followed by the addition of 25 μl of α-isonitrosopropiophenone (9% w/v), which was heated to 100°C for 45 min. OD was then read at 540-nm wavelength using a spectrophotometer (the intensity of color change of the urea–chromogen complex was measured). A standard curve was used to interpret the results by repeating the assay described above using standard stock solutions with known urea concentrations. Readings were normalized to the OD of the blank sample and water and normalized to the total protein concentration of each sample.

Western blot analysis

Western blot analysis was performed to determine the effect of macrophage polarization on the protein mediators of NF-κB and Stat1 signaling pathways. Cell lysates obtained from the polarization assay described above were quantified. Samples of 20–30 μg of protein were denatured in loading buffer (Bio-Rad Laboratories) containing 2-ME. Denatured samples were loaded onto 4–15% precast polyacrylamide gels (Bio-Rad Laboratories). Proteins were then separated by electrophoresis at 100 V for 1–2 h and transferred onto a methanol-activated and wetted Immobilon-FL PVDF membranes at 100–200 V for 90 min (LI-COR Biosciences, Lincoln, NE). The membranes were rinsed and then blocked using TBS-based Odyssey Blocking Buffer (LI-COR Biosciences). Membranes were then incubated overnight at 4°C with primary Abs specific for p65, IκBα, IKKβ, phospho-IKKβ (Abcam, Cambridge, U.K.), phospho-Stat1 (Santa Cruz Biotechnology, Dallas, TX), Stat1 (Thermo Fisher Scientific), or actin (LI-COR Biosciences) at recommended dilutions. Membranes were washed and subsequently incubated with the appropriate IRDye Subclass Specific secondary Ab (IRDye 680RD Goat anti-rabbit or IRDye 800CW Goat anti-mouse, LI-COR Biosciences). Membranes were imaged and analyzed using the Odyssey CLx Imaging System (LI-COR Biosciences). Quantification was performed using ImageJ.

IKKβ assay

A two-plate homogeneous time-resolved fluorescence (HTRF) assay was used to examine the effects of AZM on IKKβ kinase activity. The assay detects endogenous levels of IKKβ only when phosphorylated at Ser 177 and Ser 181 (31, 32). Polarized macrophages were stimulated with LPS, and cells were lysed according to manufacturer protocol (Cisbio, Codolet, France). Supernatants were removed, and cells were incubated with the supplemented lysis buffer for 30 min at room temperature with shaking. After homogenization, samples were incubated with the Ab mixture (phospho-IKKβ cryptate/phospho-IKKβ d2 Abs) for 2 h at room temperature in 384-well small-volume white plates. Fluorescence emission was then read at 665 and 620 nm using Synergy H1 plate reader. HTRF ratios are calculated by dividing the fluorescence signal at 665 nm by the fluorescence signal at 620 nm and multiplied by a factor of 10^4. Percent coefficient of variation is equal to the SD divided by the mean ration and multiplied by 100.

Statistical analysis

Statistical analysis was performed using GraphPad Prism (GraphPad Software, La Jolla, CA). Comparison between groups was made via one-way ANOVA with Tukey test multiple comparisons, paired sample *t* test with McNemar test, or via two-way ANOVA with Sidak multiple comparisons test where appropriate. Repeated measures ANOVA with Tukey multiple comparison tests were used for time-course experiments.

Results

AZM prevents p65 nuclear translocation while increasing IKKβ concentrations

We first assessed the effects of AZM on the activation of transduction proteins involved in the NF-κB signaling cascade. Macrophages

incubated overnight with IFN-γ alone or with AZM were stimulated with LPS, then fractionated into nuclear and cytoplasmic fractions to assess the effects of AZM on the translocation of p65 subunits to the nucleus. (Fig. 1). Overnight incubation with IFN-γ and stimulation with LPS (Fig. 1A) induced p65 nuclear translocation with a peak in nuclear p65 fractions at 30 min after LPS stimulation. However, AZM treatment in the presence of IFN-γ completely prevented p65 translocation to the nucleus at all timepoints. Treatment with AZM at all concentrations tested was associated with retention of p65 in the cytoplasm, shown for AZM concentrations of 5 and 30 μM. This was coupled with decreased p65 fractions in the nuclei of cells treated with AZM compared with cells treated with IFN-γ only, with the ratios of p65 nuclear to cytosolic fractions shown over time in Fig. 1B.

Additionally, immunostaining was used to visualize the localization of p65 subunits relative to the nucleus at 30 min after LPS stimulation (Fig. 2). NF-κB p65 subunits were stained with a FITC-conjugated Ab (green). The p65 signal was overlaid with the DAPI-stained nuclei (blue) to determine the localization of the subunits in the polarized macrophages (Fig. 2A). Similar to the observations in Fig. 1, a strong nuclear signal was observed in IFN-γ polarized macrophages, whereas AZM treatment was associated with a strong cytoplasmic signal. The nuclear translocation scoring (Fig. 2B) shows a significant decrease in p65 nuclear translocation with AZM treatment at all the concentrations tested compared with IFN-γ polarized macrophages. Similar results were also observed using primary BMDMs, with AZM causing blunted p65 nuclear translocation to a similar extent (Supplemental Figs. 1, 2).

The impact of AZM treatment upon the expression of NF-κB–associated proteins was then assessed. The amounts of IκBα, IKKβ, and phospho-IKKβ were measured by Western blot over time after incubation overnight with AZM and IFN-γ and stimulation with LPS, as described in *Materials and Methods* (Fig. 3A). The amount of IKKβ present in cell lysates remained relatively constant across all timepoints for the control and AZM treatment conditions but was increased at all timepoints by AZM, even before the addition of LPS (Fig. 3B). This baseline increase was sustained throughout the 60 min assay period. Similarly, AZM-polarized macrophages displayed increases in phospho-IKKβ levels compared with cells polarized with only IFN-γ through 10 min after LPS addition (Fig. 3C).

Additionally, AZM affected the degradation of IκBα in macrophages upon LPS stimulation. For cells incubated with IFN-γ, LPS caused the expected decrease in IκBα within 2 min (Fig. 3). This is due to activation of this pathway because, when IκBα is phosphorylated, it is rapidly ubiquitinated and degraded. However, AZM at concentrations of 5 μM delayed the degradation kinetics of IκBα, and at a concentration of 30 μM the drug blocked its degradation entirely, as graphically represented in Fig. 3D. Within 10 min of NF-κB activation, resynthesis of IκBα was observed in macrophages polarized with IFN-γ.

The increase in IKKβ is potentially a result of the inhibition of p65 translocation to the nucleus in AZM-polarized macrophages. Termination of the NF-κB pathway involves resynthesis of IκBα induced by the activated NF-κB as well as downregulation of IKKβ synthesis, as IKKβ gene (Ikbkb) transcription is inhibited when p65 is in the nucleus as a feedback mechanism (11, 18, 33–36). To test this, we compared mRNA expression for Ikbkb via RT-PCR and found that AZM treatment caused a modest increase as compared with the control condition (Fig. 3E). Significant differences were observed with an increase in gene expression at some timepoints including time zero; however, the increased gene

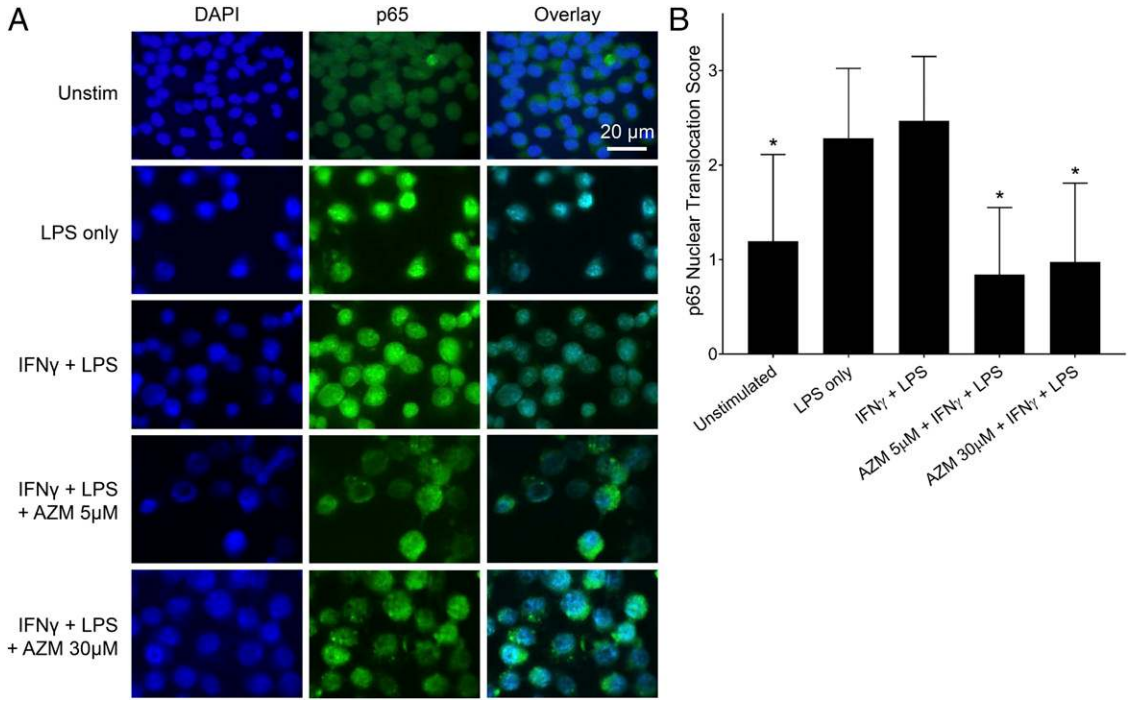

FIGURE 2. NF-κB p65 subunit accumulates in the cytoplasm around the nuclear membrane in AZM-treated macrophages. J774 murine macrophages were plated at 2.5×10^5 cells on round glass coverslips. Cells were allowed to attach to the glass and then polarized overnight with IFN-γ (50 U/ml) alone or along with AZM. Cells were then stimulated with LPS (10 nM) for 30 min. (**A**) Immunofluorescence staining for the p65 subunit of NF-κB at original magnification ×100. Images show NF-κB p65 subunits stained in green (FITC) overlaid with DAPI nuclear staining. (**B**) Bar graphs represent the nuclear versus cytoplasmic fractions of p65 quantified using a scoring system as follows: p65 signal in cytoplasm only (score 0), evenly distributed between the nucleus and cytoplasm (score 1), mostly nuclear with faint cytoplasmic signal (score 2), or nuclear signal only (score 3). Data values depict mean ± SD and are representative of three independent experiments. Statistical significance determined by two-way ANOVA, with AZM-treated groups compared with the control (IFN-γ plus LPS) condition. $*p < 0.05$.

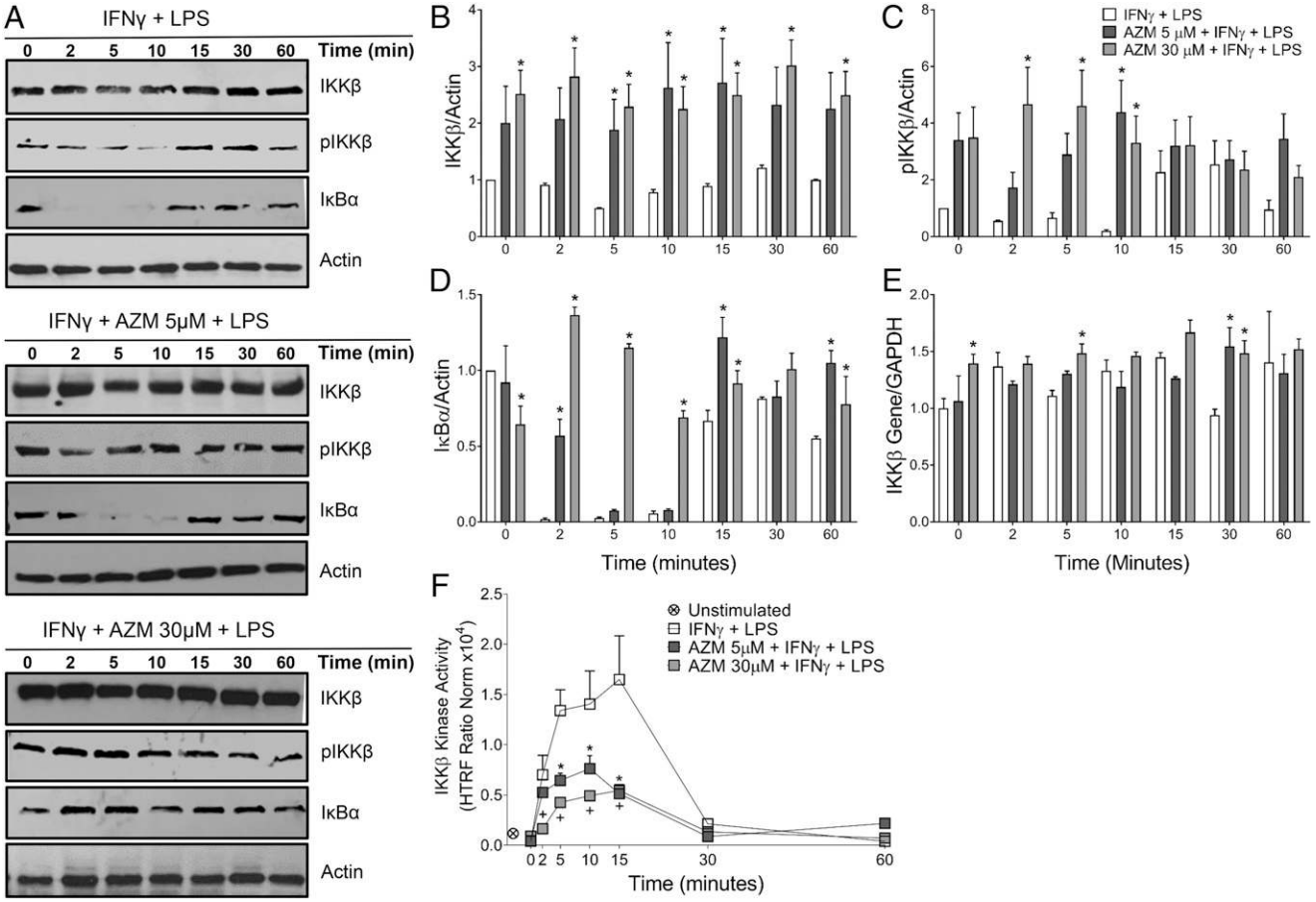

FIGURE 3. AZM prevents IκB-α degradation while accumulating IKKβ. J774 cells were plated at 2.5×10^5 cells per 1 ml of media in 24-well plates. Cells were allowed to attach for 8 h and then were polarized overnight with IFN-γ (50 U/ml) alone or along with AZM at concentrations ranging from 5 to 100 μM. Cells were then stimulated with LPS (10 nM) and harvested at timepoints between 0 and 60 min. Proteins and RNA were then collected and probed for mediators in the NF-κB signaling cascade using Western blot, RT-PCR, and HTRF assay. (**A**) Western blots depict IκB-α, IKKβ, phospho-IKKβ, and actin over time. (**B**–**D**) Relative fold change over time after LPS simulation of IKKβ, phospho-IKKβ, and IκB-α, respectively. IKKβ, phospho-IKKβ, and IκB-α band intensities were normalized to actin and the control condition at time 0. Data represents mean ± SD. $*p < 0.05$. (**E**) Relative fold change in IKKβ gene expression calculated from the ΔΔCt values, normalized to GAPDH, and compared with IFN-γ–treated macrophages at time 0. Data represents mean ± SD. $*p < 0.05$. (**F**) Changes in IKKβ kinase activity over time after LPS stimulation. HTRF ratios were calculated from the fluorescence signals at 665 and 620 nm and are representative of the kinase activity of IKKβ. Values represent mean ± %coefficient of variation. Data are representative of three independent experiments. Statistical significance was determined by two-way ANOVA with Sidak multiple comparisons test. $*p < 0.05$ AZM 5 μM, (+) AZM 30 μM and are normalized to total IKKβ and actin.

expression of Ikbkb induced by AZM was not substantial, with only moderate increases of~1.5 times control expression levels observed.

Last, because AZM blunts IκBα degradation in the presence of increased IKKβ protein expression, we sought to determine whether the drug affects IKKβ kinase activity. Activated phospho-IKKβ (Ser177/181) was detected using Abs labeled with Eu^{3+}–cryptate (donor) and d2 (acceptor). Fluorescence resonance energy transfer is triggered when the two dyes are in close proximity thus fluorescing at a specific wavelength of 665 nm. The fluorescence signal is proportional to the phospho-IKKβ at Ser177/181, which is measured as a surrogate for kinase activity. Kinase activity increased as expected after LPS stimulation in the control cells over time. AZM treatment was associated with significantly lower IKKβ kinase activity (when normalized to actin and IKKβ protein levels) between 5 and 15 min after stimulation compared with the IFN-γ polarized macrophages (Fig. 3F). By 30 min after LPS stimulation, kinase activity returned to baseline levels in all treatment groups. Similar results were demonstrated using primary mouse BMDMs polarized with AZM (Supplemental Fig. 1C).

Inhibition of IKKβ activation prevents AZM from increasing production of the M2 macrophage effector protein arginase

Because AZM increased the amount of IKKβ present, we sought to determine whether AZM exerts its effect on macrophage polarization via this mechanism. A previous report by Fong et al. (37) shows that excessive IKKβ activation prevents the induction of proinflammatory characteristics of macrophages. We treated macrophages with cytokines and AZM to polarize them into either M1 or M2 cells and added IKK-16, an inhibitor of IKKβ (Fig. 4). This inhibitor displays a high affinity for IKKβ, with an IC_{50} of 40 nM. At higher concentrations, it can also inhibit the activation of the entire IKK complex (38). Arg1 is an important effector of M2 macrophages, and it is a marker of M2 macrophage polarization induced in response to Th2 cytokines (39). AZM increased Arg1 gene expression in cells incubated with IFN-γ and exposed to LPS (Fig. 4A). The addition of the IKKβ inhibitor significantly negated the effect of AZM on Arg1 gene expression. Interestingly, the decrease in Arg1 gene expression was not statistically significant when IKK-16 was added to wells treated with IL-4 and IL-13 (the M2 control condition) ($p = 0.115$). These data suggest that AZM's

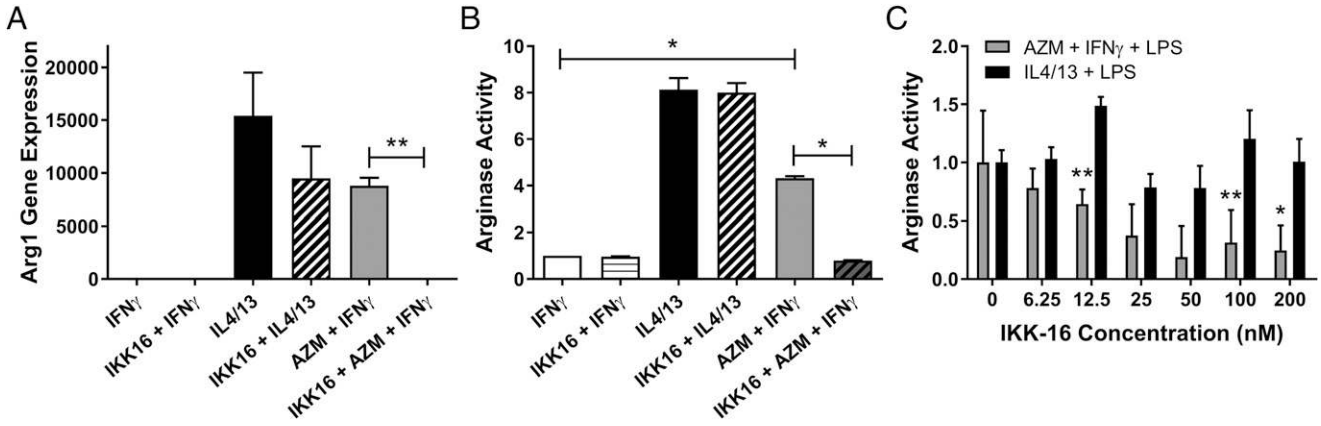

FIGURE 4. AZM-induced arginase gene expression and activity are reversed with IKKβ inhibition. J774 cells were stimulated overnight with IFN-γ, IL-4, and IL-13 or with AZM (concentration 10 μM shown in this study) plus IFN-γ in the presence or absence of the IKKβ inhibitor IKK-16. Cells were then stimulated with LPS for 24 h. (**A**) Arg1 gene expression was analyzed by quantitative RT-PCR. Bar graphs represent fold change in Arg1 gene expression calculated from the ΔΔCt values normalized to GAPDH and compared with IFN-γ–treated macrophages. (**B**) Arginase activity as determined using an enzymatic assay in lysates from polarized macrophages. Data values represent fold change in arginase activity calculated from the standard curve under different polarization conditions compared with IFN-γ–treated macrophages. (**C**) Fold change in arginase activity with increasing IKK-16 concentrations compared with no inhibitor treatment for cells treated with IFN-γ plus AZM or with IL-4/13. Data depicts mean ± SD and is representative of three independent experiments. Statistical significance was determined by two-way ANOVA. $*p < 0.05$, $**p < 0.0001$.

ability to induce expression of Arg1, an important M2 effector, is dependent on its effect on IKKβ.

We next assessed the effect of IKK-16 on arginase protein activity (Fig. 4B). In this series of experiments, cells were treated with 100 nM of IKK-16, a concentration chosen because of its maximal inhibition. Once again, AZM increased the amount of arginase activity as previously published but not to the extent of the M2 control condition of IL-4 and IL-13 treatment (6). The inhibitor had no effect on arginase activity in cells treated with IL-4 and IL-13 plus LPS, but, for the cells incubated with AZM, treatment with IKK-16 decreased arginase activity to similar levels as cells that were not exposed to the drug. When cells were treated with increasing concentrations of IKK-16, the inhibition of AZM-induced arginase activity was consistent over a wide range of concentrations, with statistically significant decreases from 12.5 to 200 nM (Fig. 4C). The inhibition of IKKβ had a little effect, however, on IL-4– and IL-13–dependent arginase production over the broad range of concentrations.

Inhibition of STAT-1 phosphorylation by AZM is dependent upon IKKβ

We then assessed the effect of AZM on the phosphorylation of STAT-1. Phosphorylated STAT-1 dimerizes and translocates to the nucleus of the cell, where it initiates the transcription of several cytokines and inflammatory genes, most of which are associated with M1 macrophage activation (11, 12). J774 macrophages were polarized under conditions to drive them to either an M1 (IFN-γ) or an M2 (IL-4/13) phenotype. IFN-γ–treated cells were also polarized in the presence of different AZM concentrations. After stimulation with LPS, we assessed the concentrations of phospho–STAT-1 and STAT-1. As shown in Fig. 5, IFN-γ activated STAT-1, leading to an increase in the phosphorylated form, whereas IL-4 and IL-13 blunted this increase in phosphorylation and resulted in lower levels of phospho–STAT-1, as expected. The LPS-alone control had similar levels of phospho–STAT-1 as the media control. AZM treatment also blunted IFN-γ–dependent STAT-1 phosphorylation, decreasing phospho–STAT-1 levels in a concentration-dependent manner. These results support our previous observation that AZM blunts NF-κB activation and subsequently shifts macrophage polarization away from the M1 phenotype. Inhibiting IKKβ via IKK-16 was associated with a reversal of AZM's effect, with the addition of IKK-16 to the AZM-polarized macrophages restoring the phosphorylation of STAT-1 (Fig. 6). Additionally, primary BMDMs polarized with AZM also show decreased STAT1 activation compared with IFN-γ polarized BMDMs, an effect which is again reversed by IKK-16 treatment (Supplemental Fig. 3).

Discussion

Macrophages constitute the first line of defense for pathogen infiltration into the lungs through their ability to initiate inflammation. This is accomplished in the case of Gram-negative pathogens primarily through the binding of TLR4 to bacterial LPS (40). NF-κB activation, through the binding of IFN-γ and LPS, leads to the transcription of inflammatory genes, including cytokines and chemokines. The NF-κB signaling cascade synergizes with STAT-1 activation to polarize macrophages to this classically activated phenotype (11, 12). In this study, we demonstrate that the immunomodulatory mechanism of AZM involves elements of both of these pathways, which results in the inhibition of the translocation of p65 to the nucleus. The production of IKKβ is also increased by the drug, which, in turn, blocks the phosphorylation of STAT-1, further increasing the expression of M2 effectors (Fig. 6).

Neutrophils migrate into infected tissues to prevent bacterial pathogen replication and spread. In chronic inflammatory lung conditions, responses to bacteria such as *P. aeruginosa*, induce exaggerated or prolonged neutrophilia, leading to pulmonary damage and fibrosis. Lung scaring is caused by excessive neutrophil elastase concentrations, an imbalance in the protease/antiprotease ratio, and a vicious cycle of excessive inflammation (41–45). Whereas many groups have demonstrated that AZM reduces NF-κB activation (30, 46–49), our previous work showed that AZM also polarizes macrophages to an M2-like phenotype, both in vitro and in vivo during *P. aeruginosa* infection (6, 7). Subsequently, we demonstrated in a mouse model of *P. aeruginosa* infection that polarizing the macrophage response to one in which the M2 phenotype predominates early in the inflammatory process reduces neutrophil influx, decreases inflammation, and reduces fibrotic changes that correlate to improved morbidity and survival (7). Other effects included decreased production of iNOS

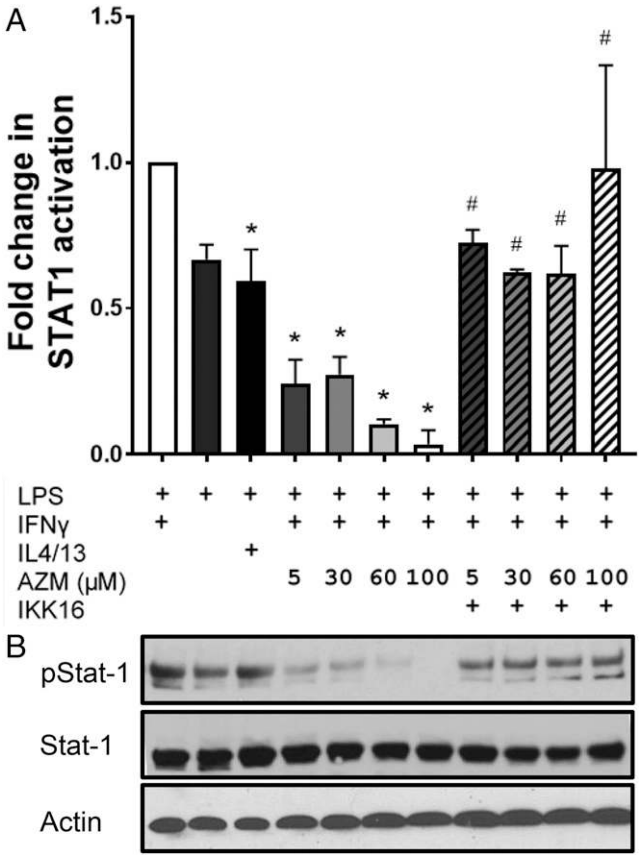

FIGURE 5. AZM prevents STAT-1 activation via an IKKβ-dependent mechanism. J774 cells were plated at 2.5×10^5 cells per 1 ml of media in 24-well plates. Cells were then polarized with IL-4 and IL-13 (10 nM each), IFN-γ (50 U/ml) alone, or with IFN-γ plus AZM (5, 30, 60, and 100 μM) with or without IKK-16 (100 nM). After overnight polarization, cells were stimulated with LPS (10 nM) for 15 min, and proteins were harvested by cell lysis. (**A**) Bar graph represents fold change in STAT-1 phosphorylation under different polarization conditions compared with IFN-γ– and LPS-stimulated macrophages (normalized to actin and STAT-1 levels) depicted by Western blot in (**B**). Western blot represents treatment conditions denoted above each lane corresponding with (A). Data depicts mean ± SD and are representative of three independent experiments. Statistical significance was determined by two-way ANOVA with Sidak multiple comparisons test. (*) denotes significant difference compared with IFN-γ + LPS and (#) denotes significant difference compared with the corresponding AZM concentration with no IKK16 treatment. $p < 0.05$.

and an increased production of the M2 effectors mannose receptor and Arg1. Our results show that lung damage is mitigated when the addition of AZM polarizes the macrophage response early in the infection (7). The efficacy of AZM in this setting is also reflected in clinical practice, as this agent is used as a chronic therapy for patients with cystic fibrosis. This is reflected in our methods to incubate cells with AZM overnight before exposing cells to LPS. Multiple clinical trials have demonstrated that quality of life is improved with chronic use of AZM, and extended treatment with AZM slows the decline of pulmonary function in patients with cystic fibrosis who are colonized with *P. aeruginosa* (50–52). We have observed in our mouse model that the clearance of *P. aeruginosa* is not altered, and, likewise, no changes in the prevalence of bacterial infection have been observed in these studies that place subjects on AZM long-term (50–52).

Additional published studies corroborate the results presented in this study. Previous reports demonstrate that the nuclear translocation of phospho-p65 is inhibited by AZM (48, 49). Additionally, Vrančić et al. (47) showed no overall impact of AZM on the phosphorylation of p65; this is consistent with our findings when factoring in the increase in phospho-p65 in the cytoplasmic fraction that we observed. They also demonstrated that AZM inhibits the phosphorylation of STAT-1. In this study, we extend these studies in our model to prove a direct relationship between increased IKKβ protein concentrations and this effect on STAT-1 through experimentally blocking IKKβ through competitive inhibition.

Evidence from the work by Fong and colleagues (37) alludes to a link between the NF-κB and STAT-1 signaling pathways. This group demonstrated that the NF-κB signaling molecule IKKβ can inhibit STAT-1 signaling in macrophages in a model of group B *Streptococcus* infection (37). Although deletion of IKKβ in airway epithelial cells led to a decrease in inflammation, macrophage-specific deletion of IKKβ caused a resistance to group B *Streptococcus* infection that was associated with increased expression of M1-associated inflammatory molecules, including IL-12, iNOS, and MHC class II (37). Additionally, in macrophages infected with group B *Streptococcus* and in macrophages incubated with IFN-γ, the absence of IKKβ led to an increase in phosphorylation of STAT-1 (37). These findings, along with our data, suggest that the increase in IKKβ expression in macrophages by AZM may be the mechanism through which polarization to the M2 phenotype occurs.

There are other examples of small molecules that inhibit the translocation of NF-κB, including aspirin, nonsteroidal anti-inflammatory drugs, and 1,8-Cineol (53–56). The nuclear binding of p65 normally provides a feedback signal to shut down the production of IKKβ (18, 57–62). Therefore, it is likely that the inhibition of p65 translocation contributes to the increase in IKKβ production. Additionally, IKKβ degradation occurs through a mechanism of autophosphorylation. Because p65 concentrations are high in the cytoplasm, this autophosphorylation process is likely decreased, which turns off the degradation pathway (32, 57, 63–67). We have shown by PCR that message expression for Ikbkb is increased; therefore, a reversal of the feedback loop is at least partly responsible. However, the difference is moderate and message expression is not increased until 30 min after LPS stimulation at lower AZM concentrations, although the IKKβ protein expression is increased earlier, even at time zero, suggesting other potential mechanisms are at work.

Despite the evidence concerning macrophage polarization, the primary immunomodulatory mechanism of AZM remains to be discovered. Clearly NF-κB activation is highly dependent upon the degradation of IκB (57, 59, 62, 68). Our data show that with higher AZM concentrations, degradation of IκBα is inhibited, leading to decreases in p65 nuclear translocation. The IκBα concentration is decreased upon stimulation with LPS for 30 min and then rebounds to baseline concentrations (Fig. 3), with p65 translocation peaking at the corresponding 30-min timepoint (Fig. 1), all of which is blocked by AZM. It is likely that the decrease in IKKβ kinase activity (Fig. 3) is a critical aspect of the drug's mechanism, which is the likely cause of the effect on IκBα, although other aspects, including proteosomal degradation, could also be affected. Additionally, the fact that p65 translocation is inhibited at time zero and by lower (5 μM) AZM concentrations provides additional evidence that other mechanisms are likely at work. This will be a focal point for future investigations.

Nuclear translocation of p65 also depends upon a number of other factors. Alteration of the nuclear location sequence of p65 can occur through a number of mechanisms, including changes in the dimerization or improper folding, which are both required. The function of importins and other nuclear shuttling machinery

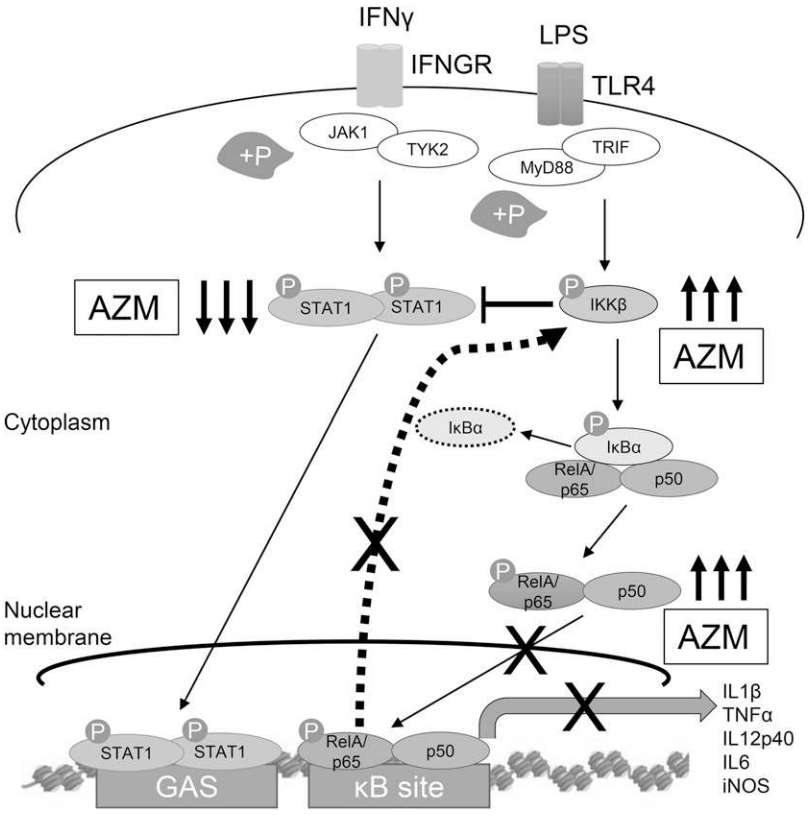

FIGURE 6. The proposed interaction induced by AZM is depicted. AZM inhibits IFN-γ–induced STAT-1 activation as well as inhibiting LPS-mediated NF-κB activation. The nuclear translocation of p65 that results in proinflammatory gene transcription is inhibited by AZM. This is due, in part, to sustained IκBα levels at higher AZM concentrations, likely stemming from decreased kinase activity of IKKβ. Because p65 nuclear translocation is inhibited at time zero and at low AZM concentrations, additional mechanisms are likely at work. Increased total IKKβ is, in part, caused by a loss of negative feedback, which otherwise shuts down the inflammatory signal by decreasing IKKβ production through decreased IKKβ gene expression. Accumulated IKKβ protein cross-inhibits the STAT-1 signaling pathway by decreasing STAT-1 phosphorylation, thereby decreasing the associated proinflammatory gene transcription and increasing the expression of the M2-associated proteins, including Arg1.

(69–71) and permeability characteristics of the nuclear membrane can be disrupted (72–77). Additionally, acetylation of the activated subunit in the nucleus at multiple lysine residues is required for translocation and is governed by histone regulation and coactivators such as CREP-binding protein (78–81). We are continuing to evaluate the impact of AZM on these mechanisms.

Future studies will investigate whether the modulation of macrophage phenotype with AZM via inhibition of the NF-κB and STAT-1 signaling pathways is beneficial in patients with cystic fibrosis. Several groups have studied the impact of macrolides, including AZM, clarithromycin, and erythromycin, on ERK1/2 and p35 MAPK signaling cascades, which result in decreased downstream NF-κB and AP-1 signaling. AZM was shown in vivo and in vitro, both in human and murine cell culture models, to decrease NF-κB activation, decrease its nuclear translocation, and decrease NF-κB and Sp1 transcription factor binding to DNA (30, 47–49, 82). These effects were associated with a significant reduction in inflammatory cell infiltration into infected lungs and a profound decrease in proinflammatory cytokine concentrations in the alveolar space. Groups studying the anti-inflammatory mechanisms of AZM show that decreases in NF-κB activation lead to suppressed induction of proinflammatory gene and protein expression in different murine and in vitro models of various inflammatory and infectious diseases (29, 30, 46–49, 82, 83). In this study, we expanded these studies to address the specific effects on the upstream mediators of the NF-κB signaling cascade and their interaction with the other inflammatory signaling pathways.

In conclusion, the immunomodulation of macrophage function by AZM is a complex effect associated with the alteration of STAT1 signaling through the inhibition of NF-κB mediators, linked through the drug's effect on IKKβ. Macrolides affect the polarization of macrophages in several models of inflammation. Studies have been extended to investigate the impact of AZM-polarized macrophages in spinal cord injury, stroke, and acute myocardial infarction (84, 85). An improved understanding of the mechanisms associated with these agents could lead to promising therapeutic target discovery in these and other devastating disease processes. And, defining interactions between signaling pathways will lead to a better understanding of cellular biology and provide the impetus for future drug discovery.

Acknowledgments

We acknowledge the expert technical assistance of Cynthia Mattingly.

Disclosures

The authors have no financial conflicts of interest.

References

1. Herbert, D. R., C. Hölscher, M. Mohrs, B. Arendse, A. Schwegmann, M. Radwanska, M. Leeto, R. Kirsch, P. Hall, H. Mossmann, et al. 2004. Alternative macrophage activation is essential for survival during schistosomiasis and downmodulates T helper 1 responses and immunopathology. *Immunity* 20: 623–635.
2. Wills-Karp, M., J. Luyimbazi, X. Xu, B. Schofield, T. Y. Neben, C. L. Karp, and D. D. Donaldson. 1998. Interleukin-13: central mediator of allergic asthma. *Science* 282: 2258–2261.
3. Reece, J. J., M. C. Siracusa, and A. L. Scott. 2006. Innate immune responses to lung-stage helminth infection induce alternatively activated alveolar macrophages. *Infect. Immun.* 74: 4970–4981.
4. Pesce, J. T., T. R. Ramalingam, M. M. Mentink-Kane, M. S. Wilson, K. C. El Kasmi, A. M. Smith, R. W. Thompson, A. W. Cheever, P. J. Murray, and T. A. Wynn. 2009. Arginase-1-expressing macrophages suppress Th2 cytokine-driven inflammation and fibrosis. *PLoS Pathog.* 5: e1000371.
5. Morty, R. E., M. Königshoff, and O. Eickelberg. 2009. Transforming growth factor-beta signaling across ages: from distorted lung development to chronic obstructive pulmonary disease. *Proc. Am. Thorac. Soc.* 6: 607–613.
6. Murphy, B. S., V. Sundareshan, T. J. Cory, D. Hayes, Jr., M. I. Anstead, and D. J. Feola. 2008. Azithromycin alters macrophage phenotype. *J. Antimicrob. Chemother.* 61: 554–560.
7. Feola, D. J., B. A. Garvy, T. J. Cory, S. E. Birket, H. Hoy, D. Hayes, Jr., and B. S. Murphy. 2010. Azithromycin alters macrophage phenotype and pulmonary compartmentalization during lung infection with *Pseudomonas. Antimicrob. Agents Chemother.* 54: 2437–2447.

8. Maarsingh, H., T. Pera, and H. Meurs. 2008. Arginase and pulmonary diseases. *Naunyn Schmiedebergs Arch. Pharmacol.* 378: 171–184.
9. Gibson, R. L., J. L. Burns, and B. W. Ramsey. 2003. Pathophysiology and management of pulmonary infections in cystic fibrosis. *Am. J. Respir. Crit. Care Med.* 168: 918–951.
10. Lyczak, J. B., C. L. Cannon, and G. B. Pier. 2002. Lung infections associated with cystic fibrosis. *Clin. Microbiol. Rev.* 15: 194–222.
11. Christian, F., E. L. Smith, and R. J. Carmody. 2016. The regulation of NF-κB subunits by phosphorylation. *Cells*. DOI: 10.3390/cells5010012.
12. Gough, D. J., D. E. Levy, R. W. Johnstone, and C. J. Clarke. 2008. IFNgamma signaling-does it mean JAK-STAT? *Cytokine Growth Factor Rev.* 19: 383–394.
13. Kovarik, P., D. Stoiber, M. Novy, and T. Decker. 1998. Stat1 combines signals derived from IFN-gamma and LPS receptors during macrophage activation. [Published erratum appears in 1998 *EMBO J.* 17: 4210.] *EMBO J.* 17: 3660–3668.
14. Locati, M., A. Mantovani, and A. Sica. 2013. Macrophage activation and polarization as an adaptive component of innate immunity. *Adv. Immunol.* 120: 163–184.
15. Wang, N., H. Liang, and K. Zen. 2014. Molecular mechanisms that influence the macrophage m1-m2 polarization balance. *Front. Immunol.* 5: 614.
16. Rath, M., I. Müller, P. Kropf, E. I. Closs, and M. Munder. 2014. Metabolism via arginase or nitric oxide synthase: two competing arginine pathways in macrophages. *Front. Immunol.* 5: 532.
17. Sun, S. C. 2011. Non-canonical NF-κB signaling pathway. *Cell Res.* 21: 71–85.
18. Oeckinghaus, A., and S. Ghosh. 2009. The NF-kappaB family of transcription factors and its regulation. *Cold Spring Harb. Perspect. Biol.* 1: a000034.
19. Koehler, D. R., G. P. Downey, N. B. Sweezey, A. K. Tanswell, and J. Hu. 2004. Lung inflammation as a therapeutic target in cystic fibrosis. *Am. J. Respir. Cell Mol. Biol.* 31: 377–381.
20. Pahl, H. L. 1999. Activators and target genes of Rel/NF-kappaB transcription factors. *Oncogene* 18: 6853–6866.
21. Ghosh, S., and M. Karin. 2002. Missing pieces in the NF-kappaB puzzle. *Cell* 109(Suppl.): S81–S96.
22. Huang, W. C., J. J. Chen, and C. C. Chen. 2003. c-Src-dependent tyrosine phosphorylation of IKKbeta is involved in tumor necrosis factor-alpha-induced intercellular adhesion molecule-1 expression. *J. Biol. Chem.* 278: 9944–9952.
23. Li, J. D., W. Feng, M. Gallup, J. H. Kim, J. Gum, Y. Kim, and C. Basbaum. 1998. Activation of NF-kappaB via a Src-dependent Ras-MAPK-pp90rsk pathway is required for Pseudomonas aeruginosa-induced mucin overproduction in epithelial cells. *Proc. Natl. Acad. Sci. USA* 95: 5718–5723.
24. Daley, J. M., T. A. Leadley, and K. G. Drouillard. 2009. Evidence for bioamplification of nine polychlorinated biphenyl (PCB) congeners in yellow perch (Perca flavascens) eggs during incubation. *Chemosphere* 75: 1500–1505.
25. Mishra, B. B., U. M. Gundra, and J. M. Teale. 2011. STAT6$^{-/-}$ mice exhibit decreased cells with alternatively activated macrophage phenotypes and enhanced disease severity in murine neurocysticercosis. *J. Neuroimmunol.* 232: 26–34.
26. Nelms, K., A. D. Keegan, J. Zamorano, J. J. Ryan, and W. E. Paul. 1999. The IL-4 receptor: signaling mechanisms and biologic functions. *Annu. Rev. Immunol.* 17: 701–738.
27. Rutschman, R., R. Lang, M. Hesse, J. N. Ihle, T. A. Wynn, and P. J. Murray. 2001. Cutting edge: Stat6-dependent substrate depletion regulates nitric oxide production. *J. Immunol.* 166: 2173–2177.
28. Weng, M., D. Huntley, I.-F. Huang, O. Foye-Jackson, L. Wang, A. Sarkissian, Q. Zhou, W. A. Walker, B. J. Cherayil, and H. N. Shi. 2007. Alternatively activated macrophages in intestinal helminth infection: effects on concurrent bacterial colitis. *J. Immunol.* 179: 4721–4731.
29. Cheung, P. S., E. C. Si, and K. Hosseini. 2010. Anti-inflammatory activity of azithromycin as measured by its NF-kappaB, inhibitory activity. *Ocul. Immunol. Inflamm.* 18: 32–37.
30. Cigana, C., B. M. Assael, and P. Melotti. 2007. Azithromycin selectively reduces tumor necrosis factor alpha levels in cystic fibrosis airway epithelial cells. *Antimicrob. Agents Chemother.* 51: 975–981.
31. Tanaka, H., N. Fujita, and T. Tsuruo. 2005. 3-Phosphoinositide-dependent protein kinase-1-mediated IkappaB kinase beta (IkkB) phosphorylation activates NF-kappaB signaling. *J. Biol. Chem.* 280: 40965–40973.
32. Delhase, M., M. Hayakawa, Y. Chen, and M. Karin. 1999. Positive and negative regulation of IkappaB kinase activity through IKKbeta subunit phosphorylation. *Science* 284: 309–313.
33. Shih, V. F., R. Tsui, A. Caldwell, and A. Hoffmann. 2011. A single NFκB system for both canonical and non-canonical signaling. *Cell Res.* 21: 86–102.
34. Moreno, R., J. M. Sobotzik, C. Schultz, and M. L. Schmitz. 2010. Specification of the NF-kappaB transcriptional response by p65 phosphorylation and TNF-induced nuclear translocation of IKK ε. *Nucleic Acids Res.* 38: 6029–6044.
35. Häcker, H., and M. Karin. 2006. Regulation and function of IKK and IKK-related kinases. *Sci. STKE* 2006: re13.
36. Hoesel, B. and J. A. Schmid. 2013. The complexity of NF-κB signaling in inflammation and cancer. *Mol. Cancer* 12: 86.
37. Fong, C. H., M. Bebien, A. Didierlaurent, R. Nebauer, T. Hussell, D. Broide, M. Karin, and T. Lawrence. 2008. An antiinflammatory role for IKKbeta through the inhibition of "classical" macrophage activation. *J. Exp. Med.* 205: 1269–1276.
38. Waelchli, R., B. Bollbuck, C. Bruns, T. Buhl, J. Eder, R. Feifel, R. Hersperger, P. Janser, L. Revesz, H.-G. Zerwes, and A. Schlapbach. 2006. Design and preparation of 2-benzamido-pyrimidines as inhibitors of IKK. *Bioorg. Med. Chem. Lett.* 16: 108–112.
39. Briken, V., and D. M. Mosser. 2011. Editorial: switching on arginase in M2 macrophages. *J. Leukoc. Biol.* 90: 839–841.
40. Mogensen, T. H. 2009. Pathogen recognition and inflammatory signaling in innate immune defenses. *Clin. Microbiol. Rev.* 22: 240–273.
41. Elizur, A., C. L. Cannon, and T. W. Ferkol. 2008. Airway inflammation in cystic fibrosis. *Chest* 133: 489–495.
42. Rao, S., and J. Grigg. 2006. New insights into pulmonary inflammation in cystic fibrosis. *Arch. Dis. Child.* 91: 786–788.
43. Nichols, D., J. Chmiel, and M. Berger. 2008. Chronic inflammation in the cystic fibrosis lung: alterations in inter- and intracellular signaling. *Clin. Rev. Allergy Immunol.* 34: 146–162.
44. Meyer, K. C., and J. Zimmerman. 1993. Neutrophil mediators, *Pseudomonas*, and pulmonary dysfunction in cystic fibrosis. *J. Lab. Clin. Med.* 121: 654–661.
45. Abboud, R. T., and S. Vimalanathan. 2008. Pathogenesis of COPD. Part I. The role of protease-antiprotease imbalance in emphysema. *Int. J. Tuberc. Lung Dis.* 12: 361–367.
46. Stellari, F. F., A. Sala, G. Donofrio, F. Ruscitti, P. Caruso, T. M. Topini, K. P. Francis, X. Li, C. arnini, M. Civelli, and G. Villetti. 2014. Azithromycin inhibits nuclear factor-κB activation during lung inflammation: an in vivo imaging study. *Pharmacol. Res. Perspect.* 2: e00058.
47. Vrančić, M., M. Banjanac, K. Nujić, M. Bosnar, T. Murati, V. Munić, D. Stupin Polančec, D. Belamarić, M. J. Parnham, and V. Eraković Haber. 2012. Azithromycin distinctively modulates classical activation of human monocytes in vitro. *Br. J. Pharmacol.* 165: 1348–1360.
48. Li, D. Q., N. Zhou, L. Zhang, P. Ma, and S. C. Pflugfelder. 2010. Suppressive effects of azithromycin on zymosan-induced production of proinflammatory mediators by human corneal epithelial cells. *Invest. Ophthalmol. Vis. Sci.* 51: 5623–5629.
49. Kanoh, S., and B. K. Rubin. 2010. Mechanisms of action and clinical application of macrolides as immunomodulatory medications. *Clin. Microbiol. Rev.* 23: 590–615.
50. Equi, A., I. M. Balfour-Lynn, A. Bush, and M. Rosenthal. 2002. Long term azithromycin in children with cystic fibrosis: a randomised, placebo-controlled crossover trial. *Lancet* 360: 978–984.
51. Saiman, L., B. C. Marshall, N. Mayer-Hamblett, J. L. Burns, A. L. Quittner, D. A. Cibene, S. Coquillette, A. Y. Fieberg, F. J. Accurso, and P. W. Campbell, III; Macrolide Study Group. 2003. Azithromycin in patients with cystic fibrosis chronically infected with *Pseudomonas aeruginosa*: a randomized controlled trial. *JAMA* 290: 1749–1756.
52. Wolter, J., S. Seeney, S. Bell, S. Bowler, P. Masel, and J. McCormack. 2002. Effect of long term treatment with azithromycin on disease parameters in cystic fibrosis: a randomised trial. *Thorax* 57: 212–216.
53. Kopp, E., and S. Ghosh. 1994. Inhibition of NF-kappa B by sodium salicylate and aspirin. *Science* 265: 956–959.
54. Yamamoto, Y., M. J. Yin, K. M. Lin, and R. B. Gaynor. 1999. Sulindac inhibits activation of the NF-kappaB pathway. *J. Biol. Chem.* 274: 27307–27314.
55. Greiner, J. F., J. Müller, M. T. Zeuner, S. Hauser, T. Seidel, C. Klenke, L. M. Grunwald, T. Schomann, D. Widera, H. Sudhoff, et al. 2013. 1,8-Cineol inhibits nuclear translocation of NF-κB p65 and NF-κB-dependent transcriptional activity. *Biochim. Biophys. Acta* 1833: 2866–2878.
56. Wong, B. C., X. Jiang, X. M. Fan, M. C. Lin, S. H. Jiang, S. K. Lam, and H. F. Kung. 2003. Suppression of RelA/p65 nuclear translocation independent of IkappaB-alpha degradation by cyclooxygenase-2 inhibitor in gastric cancer. *Oncogene* 22: 1189–1197.
57. Karin, M. 1999. How NF-kappaB is activated: the role of the IkappaB kinase (IKK) complex. *Oncogene* 18: 6867–6874.
58. Perkins, N. D., and T. D. Gilmore. 2006. Good cop, bad cop: the different faces of NF-kappaB. *Cell Death Differ.* 13: 759–772.
59. Scheidereit, C. 2006. IkappaB kinase complexes: gateways to NF-kappaB activation and transcription. *Oncogene* 25: 6685–6705.
60. Barisic, S., E. Strozyk, N. Peters, H. Walczak, and D. Kulms. 2008. Identification of PP2A as a crucial regulator of the NF-kappaB feedback loop: its inhibition by UVB turns NF-kappaB into a pro-apoptotic factor. *Cell Death Differ.* 15: 1681–1690.
61. Singh, S., and B. B. Aggarwal. 1995. Activation of transcription factor NF-kappa B is suppressed by curcumin (diferuloylmethane) [corrected]. *J. Biol. Chem.* 270: 24995–25000.
62. Gupta, S. C., S. Prasad, S. Reuter, R. Kannappan, V. R. Yadav, J. Ravindran, P. S. Hema, M. M. Chaturvedi, M. Nair, and B. B. Aggarwal. 2010. Modification of cysteine 179 of IkappaBalpha kinase by nimbolide leads to down-regulation of NF-kappaB-regulated cell survival and proliferative proteins and sensitization of tumor cells to chemotherapeutic agents. *J. Biol. Chem.* 285: 35406–35417.
63. Gupta, S. C., C. Sundaram, S. Reuter, and B. B. Aggarwal. 2010. Inhibiting NF-κB activation by small molecules as a therapeutic strategy. *Biochim. Biophys. Acta* 1799: 775–787.
64. Schomer-Miller, B., T. Higashimoto, Y.-K. Lee, and E. Zandi. 2006. Regulation of IkappaB kinase (IKK) complex by IKKgamma-dependent phosphorylation of the T-loop and C terminus of IKKbeta. *J. Biol. Chem.* 281: 15268–15276.
65. Koul, D., Y. Yao, J. L. Abbruzzese, W. K. Yung, and S. A. Reddy. 2001. Tumor suppressor MMAC/PTEN inhibits cytokine-induced NFkappaB activation without interfering with the IkappaB degradation pathway. *J. Biol. Chem.* 276: 11402–11408.
66. Israël, A. 2010. The IKK complex, a central regulator of NF-kappaB activation. *Cold Spring Harb. Perspect. Biol.* 2: a000158.
67. Jeong, J. Y., J. H. Woo, Y. S. Kim, S. Choi, S. O. Lee, S. R. Kil, C. W. Kim, B. L. Lee, W. H. Kim, B. H. Nam, and M. S. Chang. 2010. Nuclear factor-kappa B inhibition reduces markedly cell proliferation in Epstein-Barr virus-infected stomach cancer, but affects variably in Epstein-Barr virus-negative stomach cancer. *Cancer Invest.* 28: 113–119.
68. Meyer, S., N. G. Kohler, and A. Joly. 1997. Cyclosporine A is an uncompetitive inhibitor of proteasome activity and prevents NF-kappaB activation. *FEBS Lett.* 413: 354–358.

69. Theiss, A. L., A. K. Jenkins, N. I. Okoro, J.-M. A. Klapproth, D. Merlin, and S. V. Sitaraman. 2009. Prohibitin inhibits tumor necrosis factor alpha-induced nuclear factor-kappa B nuclear translocation via the novel mechanism of decreasing importin alpha3 expression. *Mol. Biol. Cell* 20: 4412–4423.
70. Xu, D., S. G. Lillico, M. W. Barnett, C. B. Whitelaw, A. L. Archibald, and T. Ait-Ali. 2012. USP18 restricts PRRSV growth through alteration of nuclear translocation of NF-κB p65 and p50 in MARC-145 cells. *Virus Res.* 169: 264–267.
71. Guzman, J. R., J. S. Koo, J. R. Goldsmith, M. Muhlbauer, A. Narula, and C. Jobin. 2013. Oxymatrine prevents NF-κB nuclear translocation and ameliorates acute intestinal inflammation. *Sci. Rep.* 3: 1629.
72. Lin, Y. Z., S. Y. Yao, R. A. Veach, T. R. Torgerson, and J. Hawiger. 1995. Inhibition of nuclear translocation of transcription factor NF-κ B by a synthetic peptide containing a cell membrane-permeable motif and nuclear localization sequence. *J. Biol. Chem.* 270: 14255–14258.
73. Torgerson, T. R., A. D. Colosia, J. P. Donahue, Y.-Z. Lin, and J. Hawiger. 1998. Regulation of NF-κ B, AP-1, NFAT, and STAT1 nuclear import in T lymphocytes by noninvasive delivery of peptide carrying the nuclear localization sequence of NF-κ B p50. *J. Immunol.* 161: 6084–6092.
74. Letoha, T., C. Somlai, T. Takács, A. Szabolcs, K. Jármay, Z. Rakonczay, Jr., P. Hegyi, I. Varga, J. Kaszaki, I. Krizbai, et al. 2005. A nuclear import inhibitory peptide ameliorates the severity of cholecystokinin-induced acute pancreatitis. *World J. Gastroenterol.* 11: 990–999.
75. Abate, A., S. Oberle, and H. Schröder. 1998. Lipopolysaccharide-induced expression of cyclooxygenase-2 in mouse macrophages is inhibited by chloromethylketones and a direct inhibitor of NF-kappa B translocation. *Prostaglandins Other Lipid Mediat.* 56: 277–290.
76. Kolenko, V., T. Bloom, P. Rayman, R. Bukowski, E. Hsi, and J. Finke. 1999. Inhibition of NF-kappa B activity in human T lymphocytes induces caspase-dependent apoptosis without detectable activation of caspase-1 and -3. *J. Immunol.* 163: 590–598.
77. Mohan, R. R., R. R. Mohan, W. J. Kim, and S. E. Wilson. 2000. Modulation of TNF-α-induced apoptosis in corneal fibroblasts by transcription factor NF-kappaB. *Invest. Ophthalmol. Vis. Sci.* 41: 1327–1336.
78. Kiernan, R., V. Brès, R. W. Ng, M. P. Coudart, S. El Messaoudi, C. Sardet, D. Y. Jin, S. Emiliani, and M. Benkirane. 2003. Post-activation turn-off of NF-kappa B-dependent transcription is regulated by acetylation of p65. *J. Biol. Chem.* 278: 2758–2766.
79. Chen, L. F., W. Fischle, E. Verdin, and W. C. Greene. 2001. Duration of nuclear NF-kappaB action regulated by reversible acetylation. *Science* 293: 1653–1657.
80. Chen, L. F., and W. C. Greene. 2004. Shaping the nuclear action of NF-kappaB. *Nat. Rev. Mol. Cell Biol.* 5: 392–401.
81. Corraliza, I. M., M. L. Campo, G. Soler, and M. Modolell. 1994. Determination of arginase activity in macrophages: a micromethod. *J. Immunol. Methods* 174: 231–235.
82. Matsumura, Y., A. Mitani, T. Suga, Y. Kamiya, T. Kikuchi, S. Tanaka, M. Aino, and T. Noguchi. 2011. Azithromycin may inhibit interleukin-8 through suppression of Rac1 and a nuclear factor-kappa B pathway in KB cells stimulated with lipopolysaccharide. *J. Periodontol.* 82: 1623–1631.
83. Iwamoto, S., T. Kumamoto, E. Azuma, M. Hirayama, M. Ito, K. Amano, M. Ido, and Y. Komada. 2011. The effect of azithromycin on the maturation and function of murine bone marrow-derived dendritic cells. *Clin. Exp. Immunol.* 166: 385–392.
84. Zhang, B., W. M. Bailey, T. J. Kopper, M. B. Orr, D. J. Feola, and J. C. Gensel. 2015. Azithromycin drives alternative macrophage activation and improves recovery and tissue sparing in contusion spinal cord injury. *J. Neuroinflammation* 12: 218.
85. Al-Darraji, A., D. Haydar, L. Chelvarajan, H. Tripathi, B. Levitan, E. Gao, V. J. Venditto, J. C. Gensel, D. J. Feola, and A. Abdel-Latif. 2018. Azithromycin therapy reduces cardiac inflammation and mitigates adverse cardiac remodeling after myocardial infarction: potential therapeutic targets in ischemic heart disease. *PLoS One* 13: e0200474.